ResearchGate

See discussions, stats, and author profiles for this publication at: https://www.researchgate.net/publication/3929983

A fault diagnosis system for heat pumps

Conference Paper · February 2001

DOI: 10.1109/CCA.2001.973840 · Source: IEEE Xplore

CITATIONS
9

READS
321

3 authors, including:

Hans P. Geering
ETH Zurich
174 PUBLICATIONS **2,622** CITATIONS

SEE PROFILE

All content following this page was uploaded by Hans P. Geering on 03 June 2014.

The user has requested enhancement of the downloaded file.

Proceedings of the 2001 IEEE International
Conference on Control Applications
September 5—7, 2001 • México City, México

A Fault Diagnosis System for Heat Pumps

David Zogg, Esfandiar Shafai, Hans P. Geering
Measurement and Control Laboratory (IMRT), Swiss Federal Institute of Technology Zurich (ETH)
CH-8092 Zurich, Switzerland, Fax: +41 1 632 11 39, e-mail: zogg@imrt.mavt.ethz.ch

Abstract-- **During the operation of heat pumps, faults like heat exchanger fouling, component failure, or refrigerant leakage reduce the system performance. In order to recognize these faults early, a fault diagnosis system has been developed and verified on a test bench. The parameters of a heat pump model are identified sequentially and classified during operation. For this classification, several 'hard' and 'soft' clustering methods have been investigated, while Fuzzy Inference Systems or Neural Networks are created automatically by newly developed software. Choosing a simple black-box model structure, the number of sensors can be minimized, whereas a more advanced grey-box model yields better classification results.**

Index terms-- **Fault detection and diagnosis for heat pumps, parameter identification, clustering, fuzzy logic and neural network classification.**

I. Introduction

A fault diagnosis system for heat pumps is presented, which contains two modules. The first module performs the parameter identification task, whereas the second module classifies the parameters and assigns them to different fault cases [20].
A number of approaches for fault detection and diagnosis have been published over the years. There are direct signal evaluations [17], the comparison to known characteristics [12], as well as model-based parity-space approaches implying the calculation of residuals, or observer-based approaches [6]. Benchmark tests show that often a combination of various approaches is required [2]. For the classification task, statistical methods such as Bayes classifiers are mentioned [18] as well as expert systems [15] and methods based on fuzzy logic or neural network techniques ([16], [4]).
This work focuses on the parameter identification method for generating fault symptoms [9]. Most faults do not affect the system in an additive manner. Rather, their effects are multiplicative, i.e., they affect the parameters directly. Parameters are tolerant of disturbances or noise and are able to contain much information in a 'compact' form. For each transient data sequence there is only one parameter set. Residuals, for example, as defined by the difference between model output and measured data, would result in a more complex 'error pattern' over the whole time interval. Therefore the classification would be more involved.
Both fuzzy inference systems (FIS) and neural networks are used as classifiers. The advantage of the fuzzy systems is their analogy to expert systems, which allow the definition of rules from expert knowledge. In this work the rules are generated automatically, but they can be viewed and edited by an expert. On the other hand, neural classifiers facilitate a very effective representation of the fault clusters in the parameter space. Here the networks are similar to radial basis function (RBF) networks, which in turn are comparable to statistical approaches with Gaussian functions.
Thus some new approaches are presented for combining the idea of parameter identification with those of fuzzy or neural network reasoning by using and enhancing different clustering methods.

II. The Test Bench

The heat pump test bench is shown in Fig. 1. The refrigerant cycle contains an additional subcooler and is modified in such a way that several faults may be simulated. The evaporator and subcooler are modified externally with additional valves for the simulation of fouling. Condenser fouling is not implemented, but it would be analogous to subcooler fouling. A list of all faults is shown in Table 1. Note that faults 5 and 6 have similar impacts on the system.
The temperatures at several positions in the refrigerant cyle ($T_1..T_8$) are measured as well as the temperatures of the heat source (T_9, T_{12}) and of the heat sink (T_{10}, $T_{11}\approx T_{13}$, T_{14}).

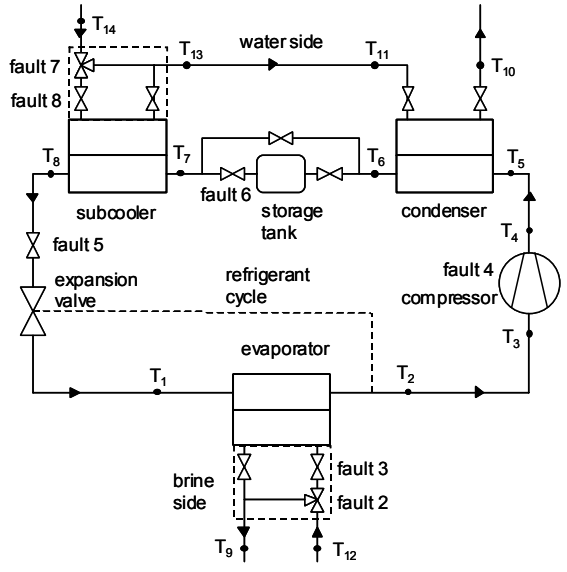

Fig. 1: Modified heat pump with 8 possible faults (fault 1 = normal behaviour). Built by the Zurich University of Applied Sciences in Winterthur.

0-7803-6733-2/01/$10.00 © 2001 IEEE

Table 1: Description of the 8 faults.

fault	actuator	fault description
fault 1	-	normal behaviour, no fault
fault 2	3-way valve	reduced evaporator heat transfer (evaporator fouling)
fault 3	valve	reduced evaporator mass flow (fouling, brine pump malfunction)
fault 4	compr. speed	reduced compressor mass flow (compressor malfunction)
fault 5	valve	reduced expansion valve mass flow (refrigerant line restriction, expansion valve malfunction)
fault 6	valve	reduced subcooler mass flow (refrigerant line restriction)
fault 7	3-way valve	reduced subcooler heat transfer (heat exchanger fouling)
fault 8	valve	reduced subcooler mass flow (fouling, water pump malfunction)

The aim of the fault diagnosis system is to classify the faults from the measured transient signals. Because the final system should be cost effective, it is important to reduce the number of sensors by finding the signals containing the highest amount of 'fault information'.

III. MODELING

For dynamically modeling the refrigerant cycle of a heat pump various approaches have been investigated, such as nonlinear modeling and linear state space modeling (eq. (1)) with underlying physical parameters θ_{ph}.

$$\begin{aligned} \dot{x} &= A(\theta_{ph})x(t) + B(\theta_{ph})u(t) \\ y &= C(\theta_{ph})x(t) + D(\theta_{ph})u(t) \end{aligned} \tag{1}$$

For an exact simulation nonlinear models would be best suited because of the nonlinearities of the evaporation and condensation processes. However, for online fault diagnosis much simpler models are required. Polynomial models (e.g., ARX models) are well suited and can be identified in a straightforward manner. The discrete time representation of the ARX model is given by eq. (2), with *e(t)* defining white noise.

$$\begin{aligned} &y(t) + A_1 y(t-1) + A_2 y(t-2) + \dots \\ &\quad = B_1 u(t-1) + B_2 u(t-2) + \dots + e(t) \end{aligned} \tag{2}$$

For the heat pump model a MIMO-ARX model is defined with the following input vectors *u(t)* and output vectors *y(t)* (with T_{11}=T_{13}).

$$y(t) = \begin{bmatrix} T_1 \\ T_2 \\ \vdots \\ T_{11} \end{bmatrix} \qquad u(t) = \begin{bmatrix} T_{12} \\ T_{14} \end{bmatrix} \tag{3}$$

Neglecting the dependence of past data prior to t-1, eq. (2) is reduced to eq. (4) or eq. (5), respectively, with A=-A_1, B=B_1, e(t)≈e(t+1).

$$y(t+1) = Ay(t) + Bu(t) + e(t) \tag{4}$$

$$y = (zI - A)^{-1} B \cdot u + (zI - A)^{-1} \cdot e \tag{5}$$

A. Physical Structure (Gray-Box Model)

The structure is called physical if the matrix *A* of eq. (4) is built on the basis of physical considerations and therefore is arbitrary. The heat pump shown in Fig. 1, with the input/output vectors of eq. (3) and an additional step input $u_{step}(t)$, yields the system matrices of eqs. (6) and (7). The additional input $u_{step}(t)$ in eq. (7) is required because the heat pump is switched on and off. For the purpose of fault diagnosis it is sufficient to consider the off-on sequence, that is a step input from 0 to 1. Consider each element • of eqs. (6) and (7) being non-zero $a_{i,k}$ or $b_{i,k}$, respectively.

$$A = \begin{bmatrix} \bullet & 0 & 0 & 0 & 0 & 0 & 0 & \bullet & 0 & 0 & 0 \\ \bullet & \bullet & 0 & 0 & 0 & 0 & 0 & 0 & \bullet & 0 & 0 \\ 0 & \bullet & \bullet & 0 & 0 & 0 & 0 & 0 & 0 & 0 & 0 \\ 0 & 0 & \bullet & \bullet & 0 & 0 & 0 & 0 & 0 & 0 & 0 \\ 0 & 0 & 0 & \bullet & \bullet & 0 & 0 & 0 & 0 & 0 & 0 \\ 0 & 0 & 0 & 0 & \bullet & \bullet & 0 & 0 & 0 & \bullet & \bullet \\ 0 & 0 & 0 & 0 & 0 & \bullet & \bullet & 0 & 0 & 0 & 0 \\ 0 & 0 & 0 & 0 & 0 & 0 & \bullet & \bullet & 0 & 0 & \bullet \\ \bullet & \bullet & 0 & 0 & 0 & 0 & 0 & 0 & \bullet & 0 & 0 \\ 0 & 0 & 0 & 0 & \bullet & \bullet & 0 & 0 & 0 & \bullet & \bullet \\ 0 & 0 & 0 & 0 & 0 & 0 & \bullet & \bullet & 0 & 0 & \bullet \end{bmatrix} \tag{6}$$

$$B = \begin{bmatrix} 0 & 0 & \bullet \\ \bullet & 0 & \bullet \\ 0 & 0 & \bullet \\ 0 & 0 & \bullet \\ 0 & 0 & \bullet \\ 0 & 0 & \bullet \\ 0 & 0 & \bullet \\ 0 & \bullet & \bullet \\ \bullet & 0 & \bullet \\ 0 & 0 & \bullet \\ 0 & \bullet & \bullet \end{bmatrix} \qquad u(t) = \begin{bmatrix} T_{12}(t) \\ T_{14}(t) \\ u_{step}(t) \end{bmatrix} \tag{7}$$

The system matrices contain all sub-models for each module of the heat pump. For example the evaporator submodel has the form of eq. (8), which corresponds to the 9th row and the columns with • of A and B.

$$\begin{aligned} T_9(t+1) &= \begin{bmatrix} a_{9,1} & a_{9,2} & a_{9,9} & b_{9,12} & b_{9,step} \end{bmatrix} \\ &\cdot \begin{bmatrix} T_1(t) & T_2(t) & T_9(t) & T_{12}(t) & u_{step}(t) \end{bmatrix}^T \end{aligned} \tag{8}$$

For other heat pump types other system structures are needed. Here the physical structure for each module and for the whole system is well represented by the model, although the model is much easier to build than it would be if an approach containing exact differential equations for the physics was used.

B. Decoupled Structure (Black-Box Model)

The structure is called decoupled if the matrix A of eq. (4) is diagonal. For the heat pump model with the input/output vectors of eq. (3) and an additional step input $u_{step}(t)$ the system is described by eq. (9).

$$\begin{bmatrix} T_1(t+1) \\ T_2(t+1) \\ \vdots \\ T_{11}(t+1) \end{bmatrix} = \begin{bmatrix} a_{1,1} & 0 & 0 & 0 \\ 0 & a_{2,1} & 0 & 0 \\ 0 & 0 & \ddots & 0 \\ 0 & 0 & 0 & a_{11,11} \end{bmatrix} \cdot \begin{bmatrix} T_1(t) \\ T_2(t) \\ \vdots \\ T_{11}(t) \end{bmatrix} + \begin{bmatrix} b_{1,12} & b_{1,14} & b_{1,step} \\ b_{2,12} & b_{2,14} & b_{2,step} \\ \vdots & \vdots & \vdots \\ b_{11,12} & b_{11,14} & b_{11,step} \end{bmatrix} \cdot \begin{bmatrix} T_{12}(t) \\ T_{14}(t) \\ u_{step}(t) \end{bmatrix} \quad (9)$$

As eq. (9) shows, there are no links among the signals $T_1..T_{11}$. This way the coherence to physics is almost lost. On the other hand we can eliminate one signal by eliminating one row as well as one column of A and one row of B without changing the other signals. This feature will be important in order to reduce the number of sensors during the signal selection task (cf. Sections IV.C and V). The input matrix B is full, which means that all signals are dependent on the heat source and heat sink input temperatures T_{12} and T_{14} as well as on the step input u_{step}.

C. Parameter Identification and Simulation

As an advantage of the ARX model the parameter identification task can be performed very simply, using the Least-Squares estimation method. By transposing eq. (2) we obtain the linear regression form in eq. (10) for MIMO systems ([13], [19]).

$$y^T(t) = \varphi^T(t) \cdot \theta + e^T(t) \quad (10)$$

$$y^T(t) = \begin{bmatrix} -y^T(t-1) & \cdots & u^T(t-1) & \cdots \end{bmatrix} \cdot \begin{bmatrix} A_1{}^T \\ \vdots \\ B_1{}^T \\ \vdots \end{bmatrix} + e^T(t)$$

For q measurements an estimation for the parameter matrix θ is calculated by building the pseudo inverse of the regression matrix ϕ^T, cf. eq. (11). The matrices Y^T and ϕ^T consist of q rows of $y^T(t_1)...y^T(t_q)$ and $\varphi^T(t_1)...\varphi^T(t_q)$.

$$Y^T = \phi^T \cdot \theta + E^T$$

$$\hat{\theta}_{LS} = (\phi\phi^T)^{-1}\phi \cdot Y^T \quad (11)$$

For each mode (off, on) or sequence (off-on, on-off), different parameter sets are identified, whereas we only use the parameter set for the off-on sequence here.

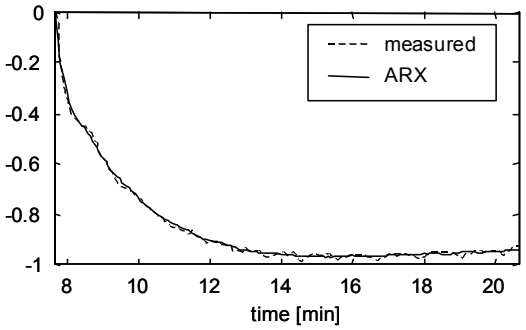

Fig. 2: Measured and simulated data from the ARX model with decoupled structure for the output signal T_9 with the inputs T_{12}, T_{14}, u_{step} (scaled signals)

Fig. 2 shows the simulation results of the ARX model with the decoupled structure after the identification of its four parameters. The evaporator brine outlet temperature T_9 plotted depends on three input signals.

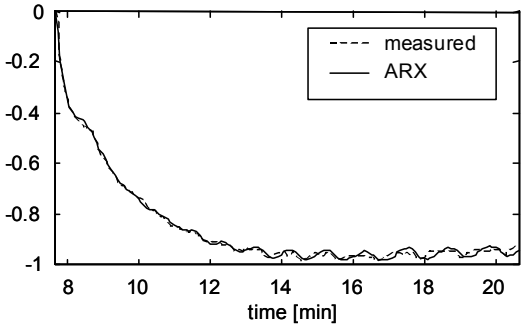

Fig. 3: Measured and simulated data from the ARX model with physical structure for the output signal T_9 with the inputs T_1, T_2, T_{12}, u_{step} (scaled signals)

The simulation results of the ARX model with the physical structure for the same signal are shown in Fig. 3. This model contains five parameters (cf. eq. (8)). Comparing it to Fig. 2 this model tries to follow the oscillations of the measured data. The oscillations are a consequence of the usual 'hunting' effect of the thermostatic expansion valve. They are most intense in the overheating temperature T_2, which is an input signal to eq. (8). Neglecting these oscillations, the decoupled model approach can be used instead of the physical approach.

IV. The Fault Diagnosis System

The system contains the parameter identification module (Section A) and the fault classification module (Section B). Similar decision making processes are suggested in [5].

A. Parameter Identification, Sensitivity Analysis

The least-squares identification method for ARX models presented in Section III.C is implemented in this module [14]. In theory, for each fault listed in Table 1 there exists one parameter set θ. But in practice we have to deal with model uncertainties, unknown inputs (disturbances, noise), and estimation errors. Thus, the estimated parameters $\hat{\theta}$ will be within a certain confidence interval for each fault.

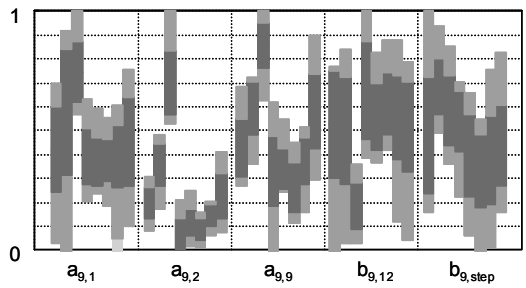

Fig. 4: Parameter values identified for the submodel of eq. (8) with the output signal T_9 and 5 parameters, for 8 different faults and 15 data points for each fault (dark grey = standard deviations, light grey = minimum/maximum, parameters scaled)

The variance of the parameters identified within one fault case and the sensitivity of the parameters to different faults is shown in Fig. 4. This bar chart may be plotted for each output signal (for each submodel) and for each parameter. All parameters are scaled to 0..1, which is important for the clustering methods presented in Section B below to work properly. The aim is to minimize variance and to maximize sensitivity. As Fig. 4 shows, there are many overlapping regions. This means that the faults cannot be separated by the values of one parameter only. Consequently, more parameters must be taken into account. The dimension n of the parameter space must be chosen such that the different fault clusters can be separated. Section C shows the solution to the problem of finding the best parameter combinations for a given number of measured signals.

B. Fault Classification

The fault classification task is performed by separating the n-dimensional parameter space into n_c clusters for each fault case. The classification system is built in two steps from measured data. In the first step the clusters are built and, based thereon, the classification system is built in the second step. Several clustering methods have been tested for a given set of data points. Sections 1) and 2) suggest 'hard' clustering methods, whereas Section 3) suggests 'soft' clustering methods. The classification system which is built in the second step can be either 'hard' or 'soft'. With a 'hard' classification a data point (parameter set) can be either inside a cluster or outside of a cluster; with a 'soft' or 'fuzzy' classification there are membership grades possible between 0 and 1. The fuzzy systems are more robust and result in fewer wrong classifications during operation. Here all the resulting classification systems are 'soft'. For the test bench introduced in Section II *HCM2Fuzzy* (Section 1)) and *HCM2Neuro* (Section 2)) yield the best results, which is the consequence of their flexible cluster shape.

1) HCM2Fuzzy Clustering

The clustering method Hard-C-means (HCM) calculates the centers and standard deviations for each cluster on each parameter axis direction (Fig. 5).

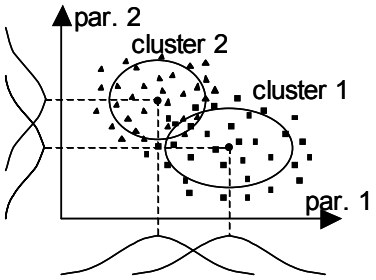

Fig. 5: Hard-C-means (HCM) clusters for two parameters and two faults with a projection onto four Gaussian fuzzy membership functions (qualitative illustration)

This clustering is called 'hard' because for the calculation of the centers each data point has the grades 1 or 0, whether or not it belongs to the cluster. On the other hand, a fuzzy classification system is built by projecting the clusters onto the axis. A Gaussian membership function for the fault i is defined by the center $c_{i,k}$ and the standard deviation $\sigma_{i,k}$ (cf. eq. (12)), x_k being the component k of a data point x.

$$f_i(x_k) = e^{\frac{-(x_k - c_{i,k})^2}{2\sigma_{i,k}^2}} \qquad (12)$$

Here the fuzzy inference system (FIS) uses the 'min' function for the AND operator as well as the implication operator, the 'max' function for the aggregation operator, and a 'centroid' defuzzification method. The membership grades of the resulting classification system for one cluster is shown in Fig. 6. Actually, there are eight fault clusters in a space of n dimensions; Fig. 6 depicts a projection of one cluster onto a plane of two dimensions. Comparing the shape of the clusters (Fig. 5 and Fig. 6) some 'projection loss' is recognizable, which is the result of the FIS operators selected. By selecting other operators (e.g., T-norm) the cluster shape could vary.

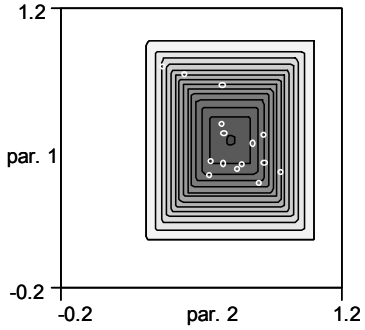

Fig. 6: HCM2Fuzzy clustering results, cut through the center of cluster 2 (fault 2) of 8 clusters, projection from n dimensions onto the first two parameter axes.

2) HCM2Neuro Clustering

The HCM clusters can also be directly included in a neural network classification system. For each cluster i the corresponding neuron transfer function is defined by eq. (13), with the cluster center components $c_{i,1}...c_{i,n}$, and the standard deviation components $\sigma_{i,1}...\sigma_{i,n}$. Setting the exponential

factor *a* to *2*, we get the extension of the Gaussian function of eq. (12) to *n* dimensions.

$$f_i(x_1 \ldots x_n) = \prod_{k=1}^{n} e^{\frac{-(x_k - c_{i,k})^2}{a\sigma_{i,k}^2}} \qquad (13)$$

Fig. 7 shows the resulting ellipsoid shape of cluster 2 with different standard deviations in either component direction. Depending on the distribution of the data points, an ellipsoid shape could match better than a 'rectangular' shape (Fig. 6). With the actual data both shapes result in a similar classification qualitiy (cf. Section V)

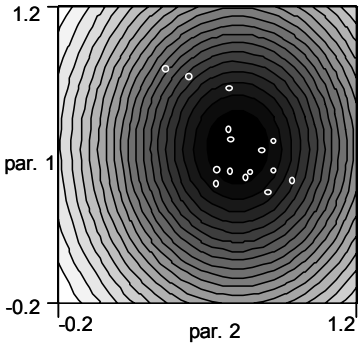

Fig. 7: HCM2Neuro clustering results, cut through the center of cluster 2

Comparing eq. (13) to the radial basis function net (RBF net) of eq. (14), we recognize that the shape of an RBF cluster would be spherical because just the distance between the data point $x=[x_1..x_n]$ and the center c_i is important:

$$f_i(x) = e^{-(\|x - c_i\| \cdot b)^2} \qquad (14)$$

RBF nets are often used for classification tasks ([11], [7]).

3) FCM2Neuro Clustering and PFCM2Neuro Clustering

The idea of this method is to use the Fuzzy-C-Means (FCM) clustering algorithm to build a classification system in which the resulting clusters are directly represented ([1], [3]). The standard 'unsupervised' FCM algorithm ([10], [8]) is designed to find clusters in a number of unclassified data points. The approach presented here uses a modified algorithm. Since the classification of the data points (i.e., the assignment of the data points to the appropriate fault clusters) is already known from experiments, the use of a 'supervised' algorithm is reasonable.

The membership grade of a point *x* regarding cluster *i* is a function of the distance d_i to the actual cluster center c_i and of the distances d_j to all other n_c centers c_j, cf. eqs. (15) and (16).

$$f_i(x) = \frac{1}{\sum_{j=1}^{n_c} \left(\frac{d_i^2(x)}{d_j^2(x)} \right)^{\frac{1}{m-1}}} \qquad (15)$$

$$d_i(x) = \|x - c_i\| \qquad (16)$$

This means that the shape of an FCM cluster *i* is influenced by all other clusters *j*.

The first step of the iterative FCM algorithm is to calculate the membership grades using eq. (15) for each cluster *i* with some initial centers c_i in eq. (16). During the next step the objective function *J* of eq. (17) is evaluated. It measures the weighted quadratic mean distance between the points and the centers. Finally the new cluster centers c_i are determined by the weighted sum of eq. (18) over $l=1..n_p$ points of each cluster.

$$J = \sum_{i=1}^{n_c} \sum_{l=1}^{n_p} f_i^m(x_l) \cdot d_i^2(x_l) \qquad (17)$$

$$c_i = \frac{\sum_{l=1}^{n_p} f_i^m(x_l) \cdot x_l}{\sum_{l=1}^{n_p} f_i^m(x_l)} \qquad (18)$$

The iteration (15) - (17) - (18) - (15) - … is stopped when the improvement of *J* between two steps is smaller than a given value ε.

In the 'supervised' algorithm the center c_i of cluster *i* in eq. (18) is calculated only from the points $l=1..n_p$ of the same cluster *i* rather than from all points. The initial centers c_i are approximated by the HCM clustering method (Secs. 1), 2)), thus by the arithmetic mean value.

The resulting FCM cluster shape in Fig. 8 is influenced by the original points of cluster 2 (small circles) as well as by the other clusters. The fewer other clusters exist next to the actual cluster, the more spherical its shape becomes.

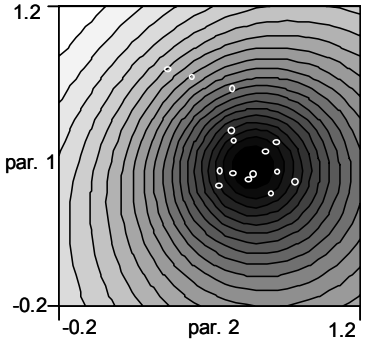

Fig. 8: FCM2Neuro clustering results, cut through the center of cluster 2

The probabilistic FCM definition of eq. (15) can be replaced by a possibilistic PFCM definition of eq. (19), which contains the parameter r_i for the extent of cluster *i*. Here the membership grades of cluster *i* are independent of other clusters.

$$f_i(x) = \frac{1}{1 + \left(\frac{d_i^2(x)}{r_i^2} \right)^{\frac{1}{m-1}}} \qquad (19)$$

A similar 'supervised' design algorithm to the one described in the case of the FCM method can be used (cf. above).

With this approach, we obtain spherical cluster shapes, as shown in Fig. 9. Thus there is a higher probability of clusters overlapping than with FCM, but the actual cluster center is only influenced by the original cluster points (small circles).

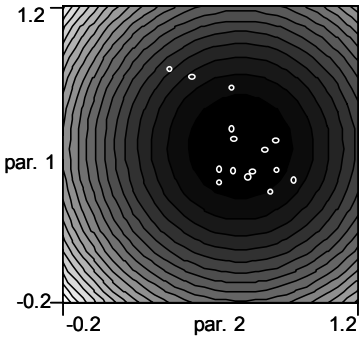

Fig. 9: PFCM2Neuro clustering results, cut through the center of cluster 2

C. Automatic System Building and Training

For the industrial realization it is important that the building and training of the fault diagnosis system is fully automated. A software tool has been developed which performs the essential steps.

During the data analysis step the measured data is separated into several off-on sequences and the parameters are identified for the selected model structure (decoupled or physical). The model errors as well as the parameter values for each fault case (Fig. 4) and for each output signal (submodel) are plotted, whereby the user can exclude some inappropriate signals in advance.

In the next step the fault clusters are created and checked. The user selects one of the clustering methods listed in Section B and chooses either single checking or multiple checking. All points of each cluster are checked for wrong classification, i.e., for cases in which the membership grade of another cluster is higher than that of the checking cluster. In the single checking mode one output signal combination is checked, whereas the multiple checking mode checks all combinations of a given number of output signals from all output signals and provides a ranking list. Moreover, the user can select different faults for each submodel. For instance fault 2 and fault 3 (Table 1) would be selected for the evaporator submodel of eq. (8). This feature empowers the physical model structure to consider the real fault input locations.

In the next step all clusters are plotted (cf. Section B) and validated. In the case of HCM2Fuzzy, the rules of the resulting FIS may be viewed or edited by an expert.

V. Experimental Results

For the heat pump test bench of Section II, various fault diagnosis systems were built by the software tool described in Section IV.C. Table 2 shows the classification quality for the physical model structure (cf. Section III.A) regarding the clustering method and the number of output signals or submodels, respectively. For each fault case, 15 data sets have been measured. Of the eight faults of Table 1 the separation of seven faults was possible with good results. Fault 5 affects the system similarly to fault 6.

Table 2: Physical model structure, number of wrong classifications for different clustering methods and output signal selections. 15 points x 7 clusters x 7 checks = 735 checks (= 100%)

method	9 output signals	3 of 9 output signals	2 of 9 output signals
HCM-2Fuzzy	4 (**0.54%**) T_2, $T_4..T_{11}$ 13 sensors	7 (**0.95%**) T_9, T_{10}, T_{11} 11 sensors	11 (**1.50%**) T_9, T_{11} 8 sensors
HCM-2Neuro	7 (**0.95%**) T_2, $T_4..T_{11}$ 13 sensors	7 (**0.95%**) T_6, T_9, T_{11} 11 sensors	11 (**1.50%**) T_9, T_{11} 8 sensors
PFCM-2Neuro	18 (2.45%) T_2, $T_4..T_{11}$ 13 sensors	18 (2.45%) T_6, T_9, T_{11} 11 sensors	22 (2.99%) T_9, T_{11} 8 sensors
FCM-2Neuro	30 (4.08%) T_2, $T_4..T_{11}$ 13 sensors	20 (2.72%) T_5, T_9, T_{11} 10 sensors	26 (3.54%) T_9, T_{11} 8 sensors

In the first column the results of the single checking procedure are presented for the nine output signals T_2, $T_4..T_{11}$, excluding the output signals T_1 and T_3 due to large model errors. The second and third columns present the results of the multiple checking procedure for three and two output signals out of nine. The output signal combinations with the best ranking (least wrong classifications) vary according to the clustering method.

Table 2 shows that HCM2Fuzzy and HCM2Neuro yield the best results with a rate of wrong classifications at or below 1.5%. PFCM2Neuro and FCM2Neuro have more wrong classifications because their shape is less flexible. Comparing HCM2Fuzzy with HCM2Neuro, the fuzzy system is slightly better. However, the computation of the fuzzy system is slower because more operators have to be evaluated (fuzzification, application of fuzzy operators, implication, aggregation, and defuzzification). The HCM methods are faster than the FCM methods, because they are non-iterative.

The number of sensors required is quite high for the physical model structure because the selected output signals depend on a number of different signals. In the case of two output signals (last column), the signal T_9 needs the signals T_1, T_2, T_{12} according to eq. (8), and T_{11} needs T_7, T_8, T_{14} according to eqs. (6) and (7), which adds up to a total of eight measured signals.

In order to reduce the number of measured signals, it is necessary to reduce the number of links to the other signals in the system matrix A. This is realized in the decoupled model structure of eq. (9) with the system matrix A being diagonal. Here the number of sensors is n_y+n_u, n_y representing the number of selected output signals and $n_u = 2$ representing the number of input signals. For all output signals we need the same two input signals T_{12} and T_{14}. As shown

in Table 3, in the case of HCM2Fuzzy the rate of wrong classifications is below 4% with five sensors and below 6% with four sensors.

Table 3: Decoupled model structure, number of wrong classifications for different clustering methods and output signal selections (735 = 100%)

method	9 output signals	3 of 9 output signals	2 of 9 output signals
HCM-2Fuzzy	29 (3.95%) T_1, T_4..T_{11} 11 sensors	29 (**3.95%**) T_6, T_9, T_{11} **5 sensors**	41 (**5.58%**) T_9, T_{11} **4 sensors**
HCM-2Neuro	27 (3.67%) T_1, T_4..T_{11} 11 sensors	32 (**4.35%**) T_6, T_9, T_{11} **5 sensors**	53 (**7.21%**) T_9, T_{11} **4 sensors**
PFCM-2Neuro	43 (5.85%) T_1, T_4..T_{11} 11 sensors	38 (5.17%) T_5, T_9, T_{11} 5 sensors	76 (10.34%) T_8, T_9 4 sensors
FCM-2Neuro	52 (7.07%) T_1, T_4..T_{11} 11 sensors	47 (6.39%) T_5, T_9, T_{11} 5 sensors	88 (11.97%) T_8, T_9 4 sensors

VI. Conclusions

For the heat pump test bench presented, the fault diagnosis system is able to handle seven different faults with a low rate of wrong classifications. The number of sensors can be minimized using a black-box decoupled model structure with the system matrix *A* diagonal. In order to minimize the number of wrong classifications, a model approach with a physical structure as well as with physically selected fault input locations proves to be most effective.

Several clustering methods have been presented for creating the fault classification system. The fast Hard-C-Means (HCM) methods yield the best results. The neural network system HCM2Neuro has a slightly worse classification quality than the fuzzy system HCM2Fuzzy, but its evaluation is faster. Both systems are related to statistical approaches using Gaussian functions, such as Bayes classifiers.

The fault diagnosis system generating process is fully automated by a software tool. There remains the experimental effort to simulate each fault case, but the modeling effort is very small.

VII. Outlook

A new test bench for industrial heat pumps will allow to obtain considerably more measured data in a shorter time. It will be fully automated in that test cycles can be defined to generate data for each fault case in the modified industrial heat pump. Both the heat source (brine cycle) and the heat sink (building) will be emulated.

A detailed nonlinear simulation model is being developed as well to generate nominal and faulty data. This model will allow the fault diagnosis system to be trained systematically for several combinations of faults and thus will act as a further test environment.

VIII. Acknowledgements

The work presented in this paper was supported by the Swiss Federal Office of Energy (BFE) within the scope of the project 'Short Time Test Method for Heat Pump Systems.' The financial support of the BFE, through the research program UAW, is gratefully acknowledged.
The support of the Zurich University of Applied Sciences Winterthur by providing their heat pump test bench is also gratefully acknowledged.

IX. References

[1] M. Ayoubi, "Fuzzy Systems Design Based on Hybrid Neural Structure and Application to the Fault Dignosis of Technical Processes," Control Engineering Practice, Vol. 4, No. 1, pp. 35-42, 1996

[2] M. Blanke and R. J. Patton, "Industrial Actuator Benchmark for Fault Detection and Isolation," Control Engineering Practice, Vol. 3, No. 12, pp. 1727-1730, 1995

[3] S. L. Chiu, "Fuzzy Model Identification Based on Cluster Estimation," Journal of Intelligent and Fuzzy Systems, Vol. 2, pp. 267-278, 1994.

[4] P. M. Frank, S. X. Ding, B. Köppen-Seliger, "Current Developments in the Theory of FDI," Preprints of 4th IFAC SAFEPROCESS Symposium, Vol. 1, pp. 16-27, 2000.

[5] P. M. Frank, "Analytical and Qualitative Model-based Fault Diagnosis – A Survey and Some New Results," European Journal of Control, pp. 6-28, 1996.

[6] J. J. Gertler, "Fault Detection and Diagnosis in Engineering Systems," Marcel Dekker, 1998.

[7] G. Guglielmi, T. Parisini, G. Rossi, "Fault Diagnosis and Neural Networks: A Power Plant Application," Control Engineering Practice, Vol. 3, No. 5, pp. 601-620, 1995.

[8] F. Höppner, F. Klawonn, R. Kruse, "Fuzzy-Cluster-analyse," Vieweg Computational Intelligence, 1997.

[9] R. Isermann, „Modellgestützte Überwachung und Fehlerdiagnose Technischer Systeme," atp Automatisierungstechnische Praxis, 5/96, 6/96. Oldenbourg, 1996.

[10] R. Jang and N. Gulley, "Fuzzy Logic Toolbox, User's Guide," The Mathworks Inc., 1999.

[11] H. N. Koivo, "Artificial Neural Networks in Fault Diagnosis and Control," Control Engineering Practice, Vol. 2, No. 1, pp. 89-101, 1994.

[12] H. v. Kuijk, "The Application of Field Characteristics to Monitor Heat Pumps for Fault Detection," Sulzer Energy Consulting, Switzerland, 1996.

[13] L. Ljung, "Systems Identification – Theory for the User," Prentice Hall, 1987.

[14] L. Ljung, "System Identification Toolbox, User's Guide," The Mathworks Inc., 1997.

[15] D. E. Maurer, "Man Machine Interface for a Failure Diagnosis Expert System," Technical Papers of IEA Annex 25, pp. 99-115, 1996.

[16] R. J. Patton, F. J. Uppal, C. J. Lopez-Toribio, "Soft Computing Approaches to Fault Diagnosis for Dynamic Systems: A Survey," Preprints of 4th IFAC SAFEPROCESS Symposium, Vol. 1, pp. 298-311, 2000.

[17] R. Räber, „Spektralmethode zur Fehlerfrüherkennung in wärmetechnischen Anlagen," Diss. ETH Nr. 12234, 1997.

[18] T. M. Rossi and J. E. Braun, "A Statistical, Rule-Based Fault Detection and Diagnostic Method for Vapour Compression Air Conditioners," HVAC&R Research, Vol. 3, No. 1, pp. 19-37, 1997.

[19] T. Söderström, P. Stoica, "System Identification," Prentice Hall, 1989.

[20] D. Zogg, „Kurztestmethode für Wärmepumpenanlagen – Phase 4: Parameteridentifikation und Fehlerdiagnose für das Teilsystem Wärmepumpe," Swiss Federal Office of Energy, 1999.

View publication stats